ICSV14

Cairns • Australia

9-12 July, 2007

14th International Congress on Sound & Vibration

INFLUENCES OF COMPRESSION EFFECT ON SOUND ABSORPTION CHARACTERISTICS

Chao-Nan Wang, Ya- Jung Lee, Yan-Min Kuo and Shih-Kai Chen

Department of Engineering Science and Ocean Engineering, National Taiwan University
1, Sec. 4, Roosevelt Road, Taipei, Taiwan, 106, ROC
wangcn@ntu.edu.tw(email address of lead author or presenter)

Abstract

The object of this research is to investigate the effect of compression on the sound absorption characteristics of a porous material. A porous material subjects to compression effect will induce the changes of density, thickness, porosity, etc. and consequently the sound absorption ability. In this work, a transfer matrix method is applied to investigate the effect of compression on sound absorption properties. The porous materials treated in this study are considered as elastic bodies rather than rigid ones. The absorption coefficients of the uncompressed and compressed porous material are initially calculated and verified from the experimental measurements. Finally the numerical predicted sound absorption coefficients for the compressed porous material are investigated.

1. INTRODUCTION

The compression effect of porous material usually occurs during carrying or installation. Thus, predicting the variation of sound absorption under compression is of interest. And that's the object of this study.

Numerous studies have applied acoustic field theory to porous materials. Allard et al. [1-3] detailed the transfer matrices of various media (acoustic, elastic, poroelastic) together with interface matrices describing the coupling between these media. A general method of modeling the propagation of sound in porous media was also presented. Additionally, Johnson et al. [4] provided the characteristic length and dynamic tortuosity of porous media to simulate the propagation of sound in porous material. Castagnede et al. [5] proposed some formulas to modify the physical parameters of porous material and thus predict the effects of compression on the absorption of sound by porous materials, but they neglected the stiffness effects of the porous materials. The solid part of a porous material was assumed to be rigid, and only the acoustic characteristics of the fluid part of the porous material were considered. However, the scheme is clearly inadequate for predicting the absorption of sound by some porous materials, as indicated in Ref. [6]. Accordingly, the solid part of a porous material should be regarded as an elastic body. In this work, Biot's theory and Castagnede's work were referenced to address both the compression effect of porous media taking into account the skeleton elasticity.

2. THEORETICAL FORMULATION

According to Allard's work [3], there can be two compression waves and one shear wave existing in a 2D porous medium. The corresponding complex wave numbers of the two compression waves, δ_1 and δ_2, are

$$\delta_1^2 = \frac{\omega^2}{2(PR-Q^2)}[P\tilde{\rho}_{22} + R\tilde{\rho}_{11} - 2Q\tilde{\rho}_{12} - \sqrt{\Delta}] \tag{1}$$

$$\delta_2^2 = \frac{\omega^2}{2(PR-Q^2)}[P\tilde{\rho}_{22} + R\tilde{\rho}_{11} - 2Q\tilde{\rho}_{12} + \sqrt{\Delta}] \tag{2}$$

where $\Delta = (P\tilde{\rho}_{22} + R\tilde{\rho}_{11} - 2Q\tilde{\rho}_{12})^2 - 4(PR-Q^2)(\tilde{\rho}_{11}\tilde{\rho}_{22} - \tilde{\rho}_{12}^2)$ and the wave number of the shear wave is

$$\delta_3^2 = \frac{\omega^2}{N}(\frac{\tilde{\rho}_{11}\tilde{\rho}_{22} - \tilde{\rho}_{12}^2}{\tilde{\rho}_{22}}). \tag{3}$$

All the definitions of the symbols can be found in Ref. [3].

The problem to be considered is shown in Fig. 1. The sound wave enters the multi-medium at side S_1 and exits from side S_2. Due to the reflection at the end of the material, six waves in a porous material should be considered simultaneously. Therefore, six independent physical parameters are required to specify the characteristics of the waves. The six chosen parameters in this work are velocities v_1^s, v_3^s, v_3^f and the stresses, σ_{33}^s, σ_{13}^s and σ_{33}^f. Then the stress and velocity relationship between M_1 and M_2 is given by

$$\mathbf{V_P}(\mathrm{M}_1) = [\mathrm{T_P}]\mathbf{V_P}(\mathrm{M}_2) \tag{4}$$

where $\mathbf{V_P} = [v_1^s \quad v_3^s \quad v_3^f \quad \sigma_{33}^s \quad \sigma_{13}^s \quad \sigma_{33}^f]^{\mathrm{T}}$ and $[\mathrm{T_P}]$ is called the transfer matrix of the porous material.

For a solid material, such as Layer 2, the solid has only two waves. Therefore, the relationship between M_3 and M_4 is given by

$$\mathbf{V}_S(\mathrm{M}_3) = [\mathrm{T_S}]\mathbf{V}_S(\mathrm{M}_4) \tag{5}$$

where $\mathbf{V}_S = [v_1^s \quad v_3^s \quad \sigma_{33}^s \quad \sigma_{13}^s]^{\mathrm{T}}$ and $[\mathrm{T_S}]$ is called the transfer matrix of the solid material. $[\mathrm{T_P}]$ and $[\mathrm{T_S}]$ are detailed elsewhere [7].

At the interfaces between media, S_1-M_1, M_2-M_3 and M_4-S_2, the boundary conditions are the continuities of the velocities and stress. Hence, the relationship between the pressures and the velocities on both sides, S_1 and S_2, can be obtained. Combining the boundary conditions at the two sides of the material yields the impedance Z_a at the incident surface S_1 [7]. Consequently, the pressure reflection coefficient $\mathrm{R_a}$ can also be determined from the surface impedance. Then, the absorption coefficient α is expressed as

$$\alpha = 1 - |\mathrm{R_a}|^2 \tag{6}$$

3. COMPRESSION EFFECT ON PARAMETERS

The compression rate n is defined as the ratio of the initial thickness d_0 to thickness d after undergoing a compression, i.e.,

$$n = \frac{d_0}{d_n} \tag{7}$$

In Eqs. (1), (2) and (3), the wave numbers are related to the parameters, tortuosity, characteristic length, flow resistivity, porosity and density. The new porosity, the flow resistivity, the tortuosity, the viscous characteristic length and the thermal characteristic length caused by the compression, are expressed as [5],

(a) Porosity $\phi^{(n)} = 1 - n(1 - \phi^{(0)})$ (8)

(b) Tortuosity $\alpha_\infty^{(n)} = 1 - n(1 - \alpha_\infty^{(0)})$ (9)

(c) Flow resistivity $\sigma^{(n)} = n\sigma^{(0)}$ (10)

(d) viscous characteristic length $\Lambda^{(n)} = \dfrac{\Lambda^{(0)}}{\sqrt{n}} + \dfrac{a}{2}(\dfrac{1}{\sqrt{n}} - 1)$ (11)

(e) thermal characteristic length $\Lambda'^{(n)} = \dfrac{\Lambda'^{(0)}}{\sqrt{n}} + \dfrac{a}{2}(\dfrac{1}{\sqrt{n}} - 1)$ (12)

The characteristic length is explained in Ref. [4].

In this work, the elastic frame is considered, in addition to the parameters mentioned above the variation in density of a porous material should also be considered.

(f) density $\rho^{(n)} = n\rho^{(0)}$ (13)

The Poisson' ratio and the bulk modulus required in the analysis remain unchanged under the linear assumption.

4. RESULTS AND DISCUSSIONS

To verify the present method, a fibrous glass panel measured by Castagnede [5] has been chosen to analyze. The values of the parameters are those of a general glass fiber used in a commercial context. Fig. 2 shows the experimental data [5] and the predicted result of the present method without any compression. Fig. 3 plots the results obtained for the compressed configuration as the thickness becomes 31 mm (n = 50/31 = 1.61). It can be seen that the agreements are good either with or without compression.

To understand the effect of the skeleton elasticity, a plastic foam studied in Ref.[6] is analyzed present method and the rigid frame approach. The thickness of the sample is 20 mm and the results for different compression rate are shown in Fig.4. It can be found that the sound absorption coefficients are different obviously. The resonance effect of the skeleton elasticity does predicted by the present method while rigid frame does not. Besides, the resonant frequency increases as the compression rate increases. Obviously the effect of the skeleton elasticity needs to be considered.

Further, three glass fibrous panels widely used in the commercial market are analyzed. Table 1 presents the properties of the material in the numerical calculation. The back plate is steel with thickness of 5.08 cm. Fig. 5 and 6 present the sound absorption coefficients of samples 24K, 32K and 48K as the thickness varies but are uncompressed. In these figures, the curves shift toward low frequency as the thickness of the porous material increases. Obviously the thick porous material has better absorption properties. Additionally, the high density of the porous material is responsible for its large absorption coefficient.

Then these samples are compressed with various compression rates. The predicted sound absorption coefficients are shown in Fig. 7, 8 and 9. In these models, the initial thickness of the uncompressed porous material is 25.4 mm. The compression rates n=1.2 and 1.5 are corresponding to materials with compressed thickness 21.17 mm and 16.93 mm, respectively. The results in these figures reveal that the sound absorption significantly decreases as the porous material is compressed. Material with different density shows the similar effect. And it can be found that thickness seems to be an important parameter.

Although the influence of thickness of a porous material on sound absorption is evident, the sound absorption coefficient in not governed only by thickness. Fibrous materials with different compression rates but with the same final thickness (25.4 mm) are analyzed. At compression rates $n = 1.2$ and 1.5, the original thicknesses of the materials are 30.4 mm and 38.1 mm respectively. Fig. 10 plots the numerical results. The large compression rate corresponds to the strong absorption of sound while the final thickness of a porous material remains constant. The compression makes the apertures of the compressed media small. The large frictional (viscous) effect of the apertures is responsible for great energy loss when sound is transmitted in the fluid part of the porous medium. Therefore, absorption coefficient of the porous material increases with the compression rate.

5. CONCLUSIONS

In this work an elastic frame is considered. The density of a porous material is modified herein. The result shows an excellent agreement between theoretical result and experimental data [1]. Further, the numerical predictions reveal that following conclusions are observed.

1. The thick porous material exhibits favorable absorption properties, when all other material properties are held constant.
2. The absorption substantially decreases because the thickness of the porous material falls under compression.
3. The large compression rate corresponds to effective absorption of sound, as the final thickness of a porous material is invariable.

Table 1 The material properties of the porous material for numerical prediction.

Sample	Density of frame ρ K (kg/m^3)	Flow resistivity σ ($Nm^{-4}s$)	Porosity φ	Shear modulus N (N/cm^2)
A1	24	8172	0.9825	10(1+0.5i)
A2	32	9140	0.9731	10(1+0.5i)
A3	48	9361	0.9627	10(1+0.5i)
	Tortuosity α_∞	Poisson coefficient ν	Viscous characteristic Λ (μm)	thermal characteristic Λ(μm)
A1	1.06	0	109	218
A2	1.06	0	107	214
A3	1.06	0	58.4	116

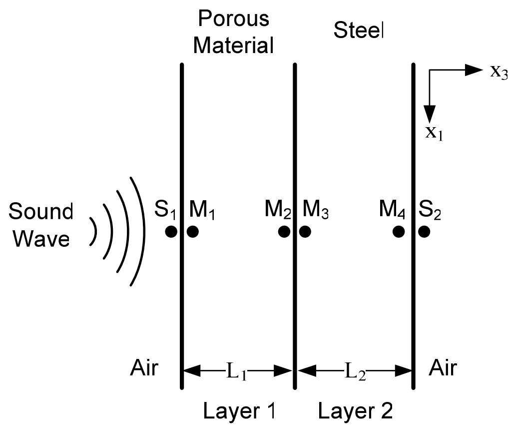

Fig. 1 The diagram of the model.

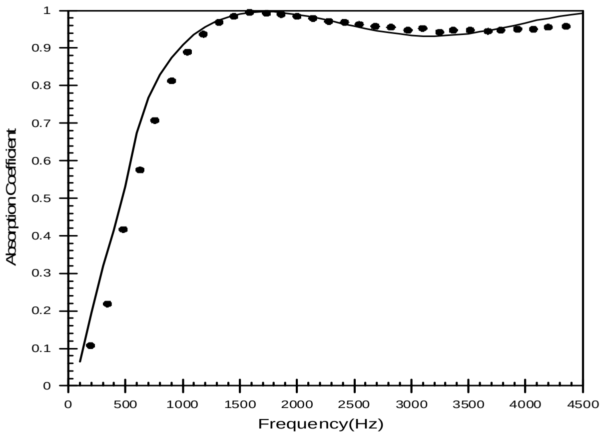

Fig. 2 The numerical simulations compared to the experimental data [1] for an uncompressed fibrous material with thickness 50 mm. Experimental data [1]: (●), present result: (——).

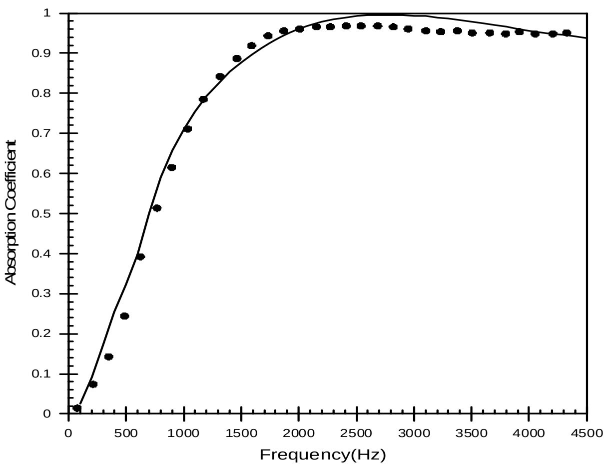

Fig. 3 The numerical simulations compared to the experimental data [1] for a compressed fibrous material with compression rate $n = 50/31 = 1.61$. Experimental data [1]: (●), present result: (——).

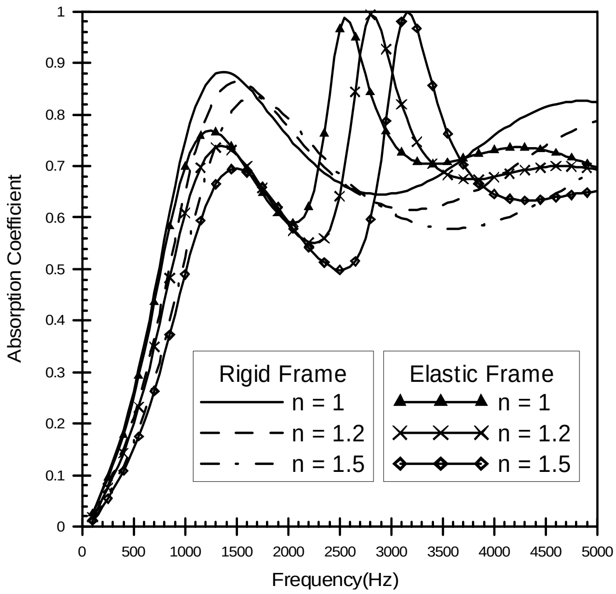

Fig. 4 Comparison of the absorption coefficient of a plastic foam studied in Ref. [6] with different compression rate. The initial thickness of the sample is 20 mm.

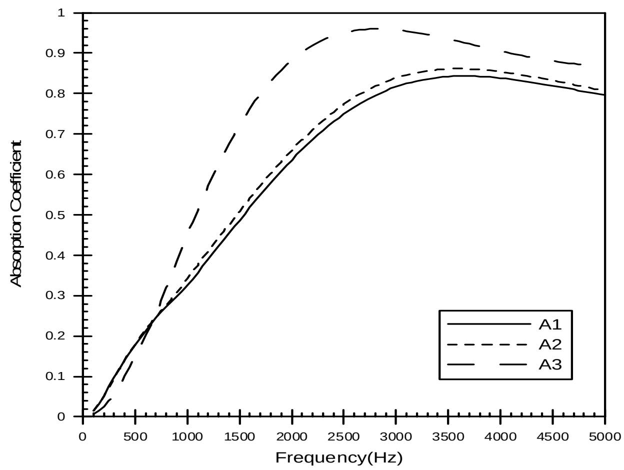

Fig. 5 The numerical simulations of the absorption coefficient of samples for uncompressed porous materials with thickness 25.4 mm. Sample A1: (——). Sample A2: (– – –). Sample A3: (— —).

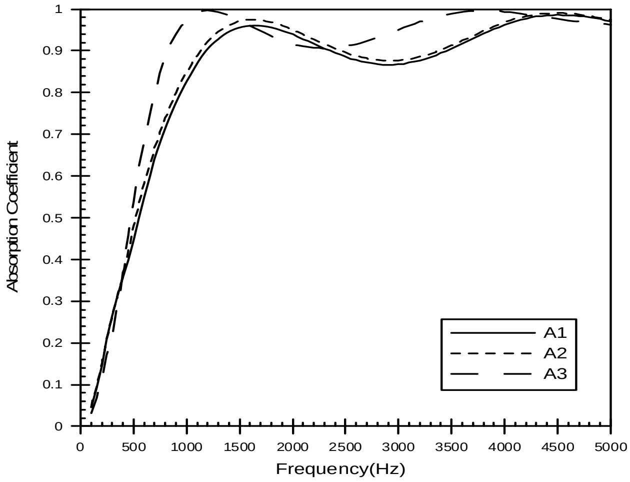

Fig. 6 The numerical simulations of the absorption coefficient of samples for uncompressed porous materials with thickness 50.8 mm. Sample A1: (——). Sample A2: (– – –). Sample A3: (— —).

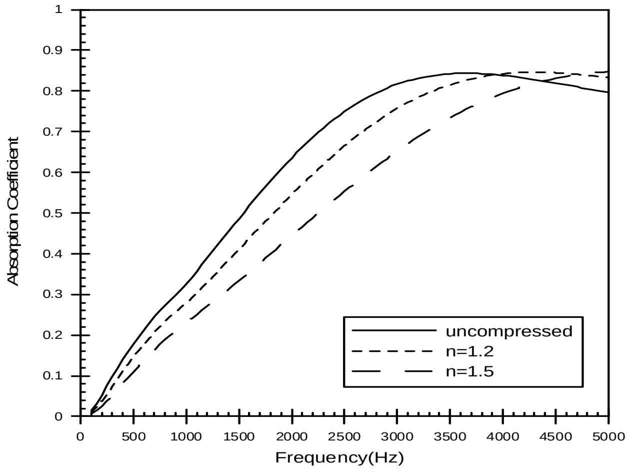

Fig. 7 The numerical simulations of the absorption coefficient of sample A1 for varying compression rate, the initial thickness of sample A1 is 25.4 mm.

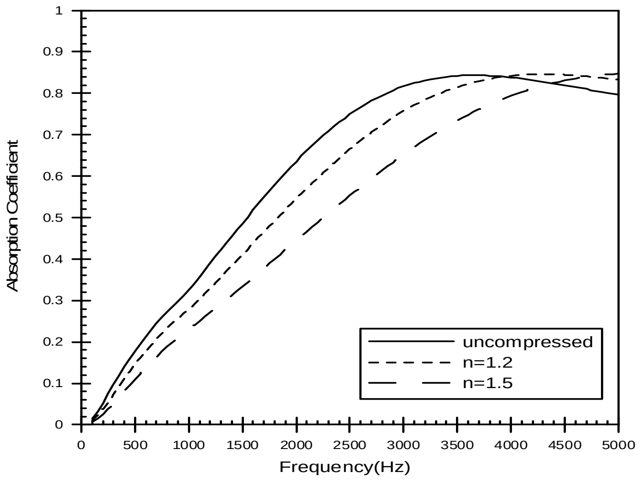

Fig. 8 The numerical simulations of the absorption coefficient of sample A2 for varying compression rate, the initial thickness of sample A2 is 25.4 mm.

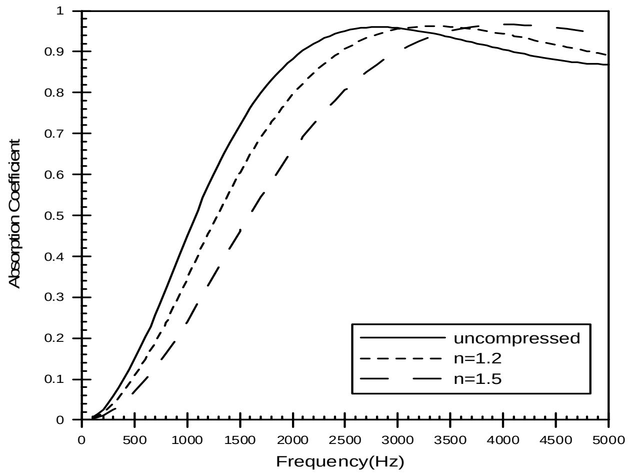

Fig. 9 The numerical simulations of the absorption coefficient of sample A3 for varying compression rate, the initial thickness of sample A3 is 25.4 mm.

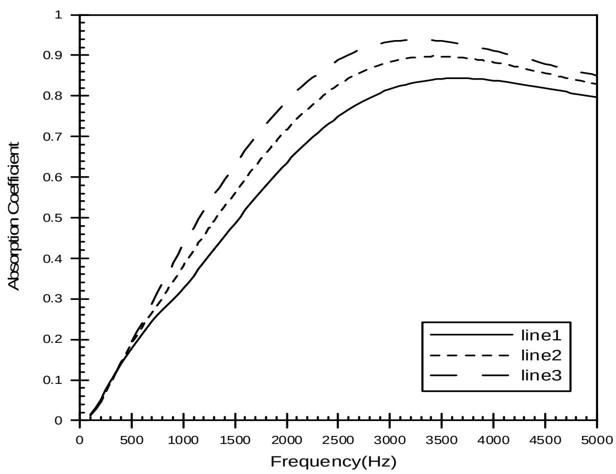

Fig. 10 The numerical simulations of the absorption coefficient of sample A2 for varying compression rate, the final thickness of sample A2 is 25.4 mm. Uncompressed, d_0 =25.4 mm, line 1: (——). Compressed, d_0 = 30.48 mm, $n = d_0 / d_n$ = 1.2, line 2: (– – –).Compressed, d_0 = 38.1 mm, $n = d_0 / d_n$ = 1.5, line 3: (— —).

REFERENCES

[1] Allard, J. F., Bourdier, R. and Depollier, C., Biot waves in layered media., J. Appl. Physics, 60, 1926-1929 (1986).

[2] Allard, J. F., Champoux, Y. and Depollier, C., Modelization of layered sound absorbing materials with transfer matrices., J. Acoust. Soc. Amer., 82, 1792-1796 (1987).

[3] Allard, J. F., Depollier, C., Rebillard, R., Lauriks, W. and Cops, A., Inhomogeneous Biot waves in layered media., J. Appl. Physics, 66, 2278-2284 (1989).

[4] Johnson, D. L., Koplik, J. and Dashen, R., Theory of dynamic permeability and tortuosity in fluid-saturated porous media., J. Fluid Mechanics, 176, 379-402 (1987).

[5] Bernard Castagnede, Achour Aknine, Bruno Brouard, Viggo Tarnow, Effects of compression on the sound absorption of fibrous materials., Applied Acoustics, v 61, n 2, 173-182 (2000).

[6] Allard, J. F., Propagation of Sound in Porous Media: Modelling Sound Absorbing Materials., Elsevier Applied Science, London (1993).

[7] Juan, C. F. and Wang, C. N. Sound insulation characteristics of panels lined with porous material. J. of Taiwan Society of Naval Architects and Marine Engineers, 23(2), 67-73, (2004).